Development of a Satellite-Based Hazard Rating System for *Dendroctonus frontallis* (Coleoptera: Scolytidae) in the Ouachita Mountains of Arkansas

STEPHEN COOK,[1] SHANE CHERRY,[2,3] KAREN HUMES,[2] JAMES GULDIN,[4] AND CHRISTOPHER WILLIAMS[5]

J. Econ. Entomol. 100(2): 381–388 (2007)

ABSTRACT The southern pine beetle, *Dendroctonus frontalis* Zimmermann (Coleoptera: Scolytidae), is the most damaging forest insect pest of pines (*Pinus* spp.) throughout the southeastern United States. Hazard rating schemes have been developed for *D. frontalis*, but for these schemes to be accurate and effective, they require extensive on-site measurements of stand attributes such as host density, age, and basal area. We developed a stand hazard-rating scheme for several watersheds in the Ouachita Highlands of Arkansas based upon remotely sensed data and a geographic information system. A hazard model was developed using stand attributes (tree species, stand age and density, pine basal area, and landform information) and was used to establish baseline hazard maps for the watersheds. Landsat 7 ETM+ data were used for developing new hazard maps. Two dates of Landsat imagery were used in the analyses (August 1999 and October 1999). The highest correlations between hazard rating scores and remotely sensed variables from either of the dates included individual Landsat 7 ETM+ bands in the near- and mid-infrared regions as well as variables derived from various bands (i.e., Tasseled cap parameters, principal component parameters, and vegetation indices such as the calculated simple ratio and normalized difference vegetation index). Best subset regression analyses produced models to predict stand hazard to southern pine beetle that consisted of similar variables that resembled but were more detailed than maps produced using inverse distance weighted techniques. Although the models are specific for the study area, with modifications, they should be transferable to geographically similar areas.

KEY WORDS southern pine beetle, Landsat ETM+, geographic information system, hazard rating

The southern pine beetle, *Dendroctonus frontalis* Zimmermann (Coleoptera: Scolytidae), is the most damaging forest insect pest of pines throughout the southeastern United States (Coulson et al. 1972). Southern pine beetle infestations, or spots, typically start small, with just a few trees being attacked and killed. However, spots may grow rapidly when environmental conditions are favorable and there is adequate resource availability (Coulson et al. 1999). Infestations of southern pine beetle can typically be found somewhere within its range every year (Payne 1980), and populations of the beetle are capable of attacking and killing all of the major species of southern pines (St. George and Beal 1929). Of the four major pine species that occur in the south, loblolly, *Pinus taeda* L., and shortleaf, *Pinus echinata* Mill., seem to be the most susceptible to attack (St. George and Beal 1929).

There are several published schemes for hazard rating forest stands for susceptibility to southern pine beetle attack (i.e., Lorio 1980b, Nebeker et al. 1995). For these schemes to effectively and accurately rate large areas, they typically require extensive on-site measurements of stand attributes such as (host density, age, and species composition of the stand). In general, as stands of pine increase in age, host density, and basal area, they become more susceptible to attack by southern pine beetle (Lorio 1980a, Flamm et al. 1988, Coulson et al. 1999). Therefore, stands that are overstocked and/or overmature are at greatest risk for infestations of the beetle to develop. Landform characteristics such as slope also may play an important role in determining stand susceptibility to southern pine beetle (Hicks 1980). Better understanding and modeling of these stand attributes can help in the development of hazard-rating schemes to enhance the effectiveness of ground and aerial survey data by focusing in on areas where activity is most likely to occur.

[1] Corresponding author: Department of Forest Resources, University of Idaho, Moscow, ID 83844-1133 (e-mail: stephenc@uidaho.edu).
[2] Department of Geography, University of Idaho, Moscow, ID 83844-3021.
[3] Current address: INEEL, P.O. Box 1625, Idaho Falls, ID 83415-2213.
[4] USDA–Forest Service, Southern Research Station, Hot Springs, AR 71902.
[5] Division of Statistics, University of Idaho, Moscow, ID 83844-1104.

Forest pest infestation and risk analysis are topic areas in which the integration of geographic information systems (GIS) and satellite-based remote sensing applications could be useful for addressing forest health issues. Remotely sensed data has been used to examine various features of a forest, including species composition (Martin et al. 1998), age (Kimes et al. 1996), and structural attributes (Cohen and Spies 1992, Bowers et al. 1994). Different vegetation types have variations in their respective spectral properties and changes in plant physiology due to increases in age, senescence, or stress that can affect these spectral properties (Mather 1996). Many of these attributes such as age and stand composition are directly related to the stand level information required for rating stands for susceptibility to southern pine beetle attack. Values derived from remotely sensed imagery such as the simple ratio (SR) and the normalized difference vegetation index (NDVI) also can provide statistically significant results for parameters such as stand basal area, volume, and tree diameter (Franklin and Luther 1995). Furthermore, remotely sensed data have been used to detect and quantify bark beetle infestations (Rencz and Nemeth 1985; Murtha and Wiart 1989; Everitt et al. 1997a,b). By combining the relatively quick and cost-effective data available from satellite-based systems such as Landsat 7 with the data storage, processing, analysis and display properties provided by current GIS (Lang 1998), a predictive tool for determining stand susceptibility to southern pine beetle infestation should be feasible. If stands can be accurately rated for risk to southern pine beetle by using remotely sensed data, it should decrease both the time and expense required to assess susceptibility over large areas. Such a technique also could be used to refine the area to be used for spring trapping of the beetle, one technique currently used to predict the short-term potential for beetle outbreaks to occur (Billings 1988).

The objective of this project was to determine whether a hazard-rating scheme could be developed for southern pine beetle in the Ouachita Mountains of Arkansas based upon remotely sensed data and a GIS.

Materials and Methods

Study Area. The study was conducted in the highlands of the Ouachita National Forest in west central Arkansas. The Ouachita highlands are narrow-topped mountains with east-to-west running ridges that range in height from ≈163 to 529 m and have slopes ranging from 0 to 41%. The average stand within the area contains ≈798 trees per hectare, with the majority of the conifer component being comprised of shortleaf and loblolly pines and the deciduous component being primarily white and southern red oaks (Guldin et al. 1994). The conifer component accounts for ≈51% of the total trees and 75% of the total basal area within the stands.

Ground Measurements. Intensive ground surveys were conducted on four watersheds from 1995 through 1998. The four watersheds were located in the Winona North Alum basin (North Alum Creek, Bread Creek, and South Alum Creek watersheds) and the nearby Little Glazypeau watershed. There were a total of 2,012 sample points from which data were collected. The data included measurements of basal area, stem density, and diameter classes based on 2.5-cm increments for the shortleaf pines, loblolly pines, other conifer species, white oaks and southern red oaks, other oaks, and other hardwood species within the plots. The data were arranged by sample year, watershed, and transect line. Coordinates for each sample plot were in the Universal Transverse Mercator projection with North American Datum 1927. The data were imported into ArcView Environmental Systems Research Institute (1998) and converted into a shape file. The mean diameter of the conifer component, the density, and basal area of host trees and the percentage of trees within a plot that were host species were calculated. Slope values for each sample plot were derived from U.S. Geological Survey (USGS) digital elevation models (DEMs at 1:24,000 scale).

Hazard Model. There was not an existing model that could readily incorporate our available stand characteristic data. Therefore, we developed a model based upon the criteria most frequently used in previous studies such as tree species present, stand age and density, basal area of the pine and hardwood components, and landform information (Coulson 1979; Lorio 1980a,b, Hicks et al. 1987; Flamm et al. 1988). Our model combined species composition within each sample plot, tree diameter data, stand density measurements, and slope. The density of trees within each sample plot was obtained directly from the ground measurements. As stand (and pine) density increased, the hazard rating for southern pine beetle also increased. Tree diameter data were used as a surrogate for stand age. Diameters were used because we did not have a direct measure of stand age and southern pine beetle does prefer mature trees with thick bark, which are characteristics consistent with large diameter trees (for examples, see Lorio 1978, Lorio and Sommers 1981, Hicks et al. 1987). As pine diameters increased, the hazard rating for southern pine beetle also increased. The slope for each sample plot was used in the hazard rating, because previous work has demonstrated that southern pine beetle prefers stands in low-lying areas and on ridge-tops but does not prefer stands on side- or steep slopes (Hicks 1980). Therefore, low slope measurements would correspond with higher hazard rating for southern pine beetle.

The model we used resulted in a possible hazard value rating of from 0 to 4.4, with 0 representing no potential risk of southern pine beetle infestation (i.e., there were no host trees present within the sample plot). The model was designed so that all input parameters had similar values, ranging from 0 to 1, with the higher values indicating higher hazard. The mathematical combination of the input parameters was constructed to ensure host presence for any hazard >0. The model we used to rate each of the sample plots for hazard of infestation by southern pine beetle was follows:

Table 1. Landsat 7 ETM+ bands used in the hazard rating analyses for southern pine beetle in the Ouachita Mountains of Arkansas

Landsat band	Wavelength	Description
1	0.45–0.52	Visible (blue)
2	0.52–0.60	Visible (green)
3	0.63–0.69	Visible (red)
4	0.76–0.90	Near-infrared
5	1.55–1.75	Mid-infrared
7	2.08–2.35	Mid-infrared
Panchromatic	0.50–0.90	

$$\text{Hazardrating} = \text{ConBA}(\text{ConDen} + \text{ConDiam} + \text{InvSlope}) \quad [1]$$

where ConBA is the proportion of the total stand basal area represented by conifers; ConDen is 0, 0.33, 0.66, or 1 for conifer densities of 0, >0 but ≤250, >250 but ≤1,000, and >1,000 stems per hectare, respectively; ConDiam is mean diameter at breast height of the conifer component/10; and InvSlope is 1/(slope + 1).

A grid representing the hazard values was then interpolated at each sample point by applying an inverse distance weighted algorithm by using ArcView. The grid was reclassified into four hazard classes representing hazard ratings of 0 (no hazard), 0.001–1.000 (low hazard), 1.001–1.500 (moderate hazard), and >1.500 (high hazard).

Remotely Sensed Imagery. Landsat 7 Enhanced Thematic Mapper Plus (ETM+) imagery was used. Bands 1–5 and 7 from the Landsat 7 ETM+ were used for this analysis (Table 1). Two dates of imagery (3 August 1999 and 22 October 1999) were used. Ideally, the two dates for the imagery would have been further apart, but due to image availability and cloud cover, the two images used represented the best combination available. The differences in spectral response between the two dates, based upon the changing deciduous tree component within the area, could thus be compared to determine which of the imagery dates provided the better information to be used to predict southern pine beetle hazard.

A subset of the Landsat 7 ETM+ imagery was fit to the boundaries of the study areas for each of the two dates. The resulting images were then georeferenced to the Universal Transverse Mercator (UTM) projection with North American Datum 1927 by performing an image to image registration using 1:24,000 digital orthophoto quadrangles (DOQ) as the reference image. A nearest neighbor resampling technique was used for the georeferencing to preserve the original image values from the unaltered scene (Campbell 1996, Mather 1996). After the georeferencing, all of the resulting images used for the analysis had root mean square errors of <8 m.

Conversion of Image Data to At-Satellite Reflectance. The raw data associated with the individual Landsat bands may not be directly comparable among scenes from different dates due to differences in such factors as sun angle, terrain, surface cover, and sensor calibration. Inconsistencies among images can be minimized by converting the raw digital values to quantitative physical values such as radiance or ground reflectance (Robinove 1982). Therefore, the imagery used for the current analysis was converted to reflectance values by using previously defined equations (Markham and Barker 1986). The image values were converted to radiance values using the following formula:

$$L_\lambda = \text{QCAL}((LMAX_\lambda - LMIN_\lambda)/\text{QCALMAX}) + LMin_\lambda \quad [2]$$

where L_λ is spectral radiance in milliwatts per square centimeter per steradian per micrometer; QCAL is calibrated and quantized scaled radiance in digital numbers units, QCALMAX is range of rescaled radiance in digital numbers, $LMin_\lambda$ is spectral radiance at QCAL = 0 from image calibration parameter file, and $LMAX_\lambda$ is spectral radiance at QCAL = QCALMAX from image calibration file.

The resulting parameters were then converted to at-satellite reflectance values as follows:

$$\rho_p = (\pi \times L_\lambda \times d^2)/\text{ESUN}_\lambda \times \cos\theta_s) \quad [3]$$

where ρ_p is unitless effective at-satellite planetary reflectance, L_λ is spectral radiance (from equation 2), d is Earth–sun distance in astronomical units (from nautical handbook), ESUN_λ is mean solar exoatmospheric irradiances (from image calibration parameter file), and θ_s is solar zenith angle in degrees.

The conversion of the image data to radiance and at-satellite reflectance values was applied to the imagery by using the modeler function in Imagine 1999.

Image Comparison between Dates. Variations in atmospheric characteristics also can have an impact on the results of the digital image analysis. Therefore, when multiple dates of imagery are used for comparisons, the data should be normalized so as to minimize the atmospheric effects (Jensen 1996). No atmospheric data were available that were temporally and spatially acceptable to the image acquisition periods. Therefore, we used a previously described method (Hall et al. 1991) to determine the need to normalize the two dates of imagery used in the analysis. At-satellite reflectance values for each of the bands used were recorded for each normalization target. Regression analysis was applied to each band in the August image to predict the normalized reflectance values for the October image. There was little difference between the actual at-satellite reflectance values and the predicted at-satellite reflectance values (Fig. 1), indicating a minimal change in the spectral response of the normalization targets between the two images. Therefore, no normalization was applied to the imagery for the analysis.

Variables Used in Hazard Rating. Hazard rating schemes were developed using two methods. The first method used variables derived directly from the remotely sensed data to directly predict stand hazard to southern pine beetle infestation. The second method used the remotely sensed data to derive individual

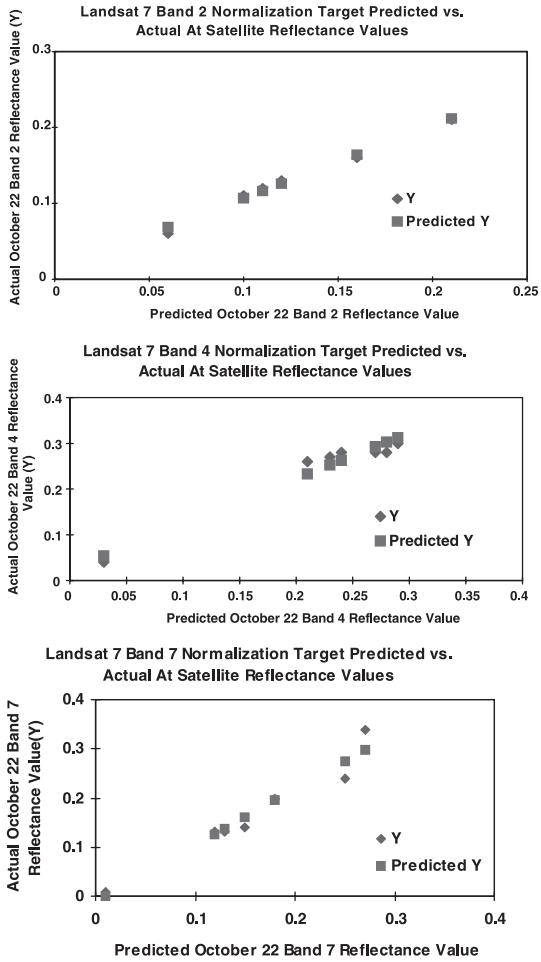

Fig. 1. Actual and predicted normalization target reflectance values for Landsat 7 ETM+ bands 2, 4, and 7 for the 22 October 1999 imagery. Predicted values for each band were derived from the regression analyses conducted for the 3 August 1999 imagery and accompanying each plot.

characteristics of the stands that were then used as input into a hazard rating scheme.

The six reflective bands from Landsat seven ETM+ (Table 1) were examined as was the difference in reflectance values for band 4 between the two dates of imagery. Combinations of the individual reflective bands were calculated and used in the analyses. One of the indices used was the SR developed by Birth and McVey (1968) and calculated as follows:

$$SR = NIR/Red \quad [4]$$

where NIR is the band representing the near-infrared portion of the electromagnetic spectrum, and Red is the band representing the red portion of the electromagnetic spectrum.

Each sample date and the difference in SR between the two sample dates were examined. The NDVI (Rouse et al. 1974) uses the same spectral band measurements and is similar to the SR values, but it effectively normalizes the difference between the NIR and red values and avoids the potential problems of the index values increasing without bounds (Chen 1996). Therefore, we also included NDVI and the difference in NDVI between the two image dates in our analyses. The NDVI values were calculated as follows:

$$NDVI = (NIR - Red)/(NIR + Red) \quad [5]$$

Tasseled cap (TC) linear transformation indices also were included in the analyses to examine brightness (TC1 is a weighted average of all six reflective bands), greenness (TC2 is a contrast between the visible and NIR bands) and wetness (TC3 is a contrast between the mid-infrared and the combined red and NIR bands) (Crist and Cicone 1984). Similarly, principal components analysis was used to create new components that were linear combinations of the original reflective bands. We used only the first three principal components from each image date in this analysis because the first component contains the greatest amount of total variance and the variance decreases with each subsequent component (Chavez and Kwarteng 1989).

Textural analysis (also referred to image textures [Campbell 1996]) was used to measure the tonal variability within a neighborhood of pixels. An available standard deviation texture algorithm (Imagine 1999) was applied to band three and band four for both image dates using a 3 by 3 pixel moving window. The algorithm was also applied to the panchromatic band from each date using both a 3 by 3 moving window and a 5 by 5 moving window. The algorithm also was applied to the linear resolution DOQ imagery using both a 3 by 3 and a 7 by 7 moving window.

An unsupervised classification was performed using the iterative self-organizing data analysis technique (ISODATA) (ERDAS, Inc. 1999), which generates a user-defined number of classes by iteratively progressing through the image and identifying distinct classes. We combined the watersheds for this step and produced an image containing five classes. The technique has been successfully used to map insect-caused defoliation (Hall et al. 1991).

Three variables that described various aspects of the terrain (elevation, slope, and aspect) were used in the analyses. The three terrain variables were derived in ArcView from the USGS DEMs described previously.

The images representing the remotely sensed variables used in this project were converted to grids so that the values corresponding to each sample plot could be extracted using the Grid format (ArcInfo, version 7.1.2, Environmental Systems Research Institute 1997) with the bilinear interpolation resampling technique. All of the data were matched with the corresponding hazard value derived from equation 1 for the corresponding sample point.

Data Extraction and Statistical Analysis. Correlation analysis (Ott 1993) was conducted to measure the linear relationship between hazard values and stand characteristics and the remotely sensed variables extracted from each date of imagery. Multiple linear

regression techniques (Ott 1993) were used to construct models to predict the hazard rating values by using the data from the two dates of imagery as the model parameters. Eighty-five percent of the data from each watershed were used as the training set for model development. Using these training sets, a best subset regression procedure was applied. The best subset regression (Ott 1993) was used to avoid running all possible regression combinations for predicting hazard values. The R^2 values were specified as the criterion for determining the best five regression models, whereas the C_p statistic and the root mean square error term were used to ensure selection of the best possible model. The best fitting model should have a C_p value approximately equal to the number of parameters in the model (Ott 1993). Once the best fitting model was selected, the remaining 15% of the data points were used to validate input for the selected models. The variance inflation factor was used to examine each of the input parameters following model selection to examine possible collinearity among the parameters (DiIorio 1997). When variables with a high degree of collinearity were detected, they were removed from the model. Once the final model was selected, the R^2 values from the original output model and the validation set model were compared to determine how well the model predicted the hazard rating scores. If the model represents an adequate fit, the R^2 value from the validation set will be similar to the R^2 value of the training set. All statistical analyses were conducted using SAS (SAS Institute 2000). For the models used to predict hazard values, the regression coefficients associated with each parameter were applied to their respective grids. The resulting grid values were added together to produce hazard maps (one map using the 3 August 1999 data, and the other map using the 22 October 1999 data). The two hazard maps were compared with the original hazard map produced using the ground survey data by examining the spatial patterns of each hazard class.

Results and Discussion

Of the variables examined using only the 3 August Landsat data, Landsat 7 ETM+ band 4 (near-infrared), tasseled cap 2 (greenness index), tasseled cap 1 (wetness index), and the first two principal components had the five highest correlation values with the calculated hazard scores (Table 2). The analysis conducted with the 22 October Landsat data included measurements of the difference between the 22 October Landsat data and the 3 August Landsat data for the vegetation indices, NDVI and SR. Along with Landsat 7 ETM+ band five values (mid-infrared), the first principal component values, and the tasseled cap 1 values (wetness index), both of these difference values for the vegetation indices had the highest correlation values with the calculated hazard scores (Table 2). The major difference in the data from the two acquisition dates seems to be contained in the measurements concerned within the near-infrared range. The areas used in this project are mixed pine–deciduous hardwood forests. Although the hazard rating values were based on attributes associated with the pine component of the stands, the deciduous hardwood component would have affected the measured spectral signatures. The Landsat data from 3 August was acquired when the deciduous component of the stands still contained green foliage. Therefore, the Landsat data from the 3 August scene would include a higher proportion of hardwood foliage in the spectral measurements. Previous studies have reported that the deciduous component of a mixed forest can dominate measurements of spectral response when attempting to measure the attributes of conifers in a mixed forest (Ahern et al. 1991, Franklin and Luther 1995). As the foliage begins to dry and change color, there is less chlorophyll contained in the inner leaf tissue that drives the high near-infrared spectral response of healthy, vigorous vegetation (Mather 1996, Jensen 2000). Because these phenological changes occur within trees/forest stands during the autumn, the spectral signature acquired will be different from that acquired from the same trees/forest stands during the summer. Furthermore, as the deciduous component of a stand begins to drop its foliage, spectral signatures may be influenced by soil properties that were not evident when the foliage was still on the trees.

Table 2. The seven highest correlation coefficient values between the southern pine beetle hazard-rating scores for stands in four watersheds in the Ouachita Mountains of Arkansas and data derived from the remotely sensed imagery from two sample dates

Imagery acquisition date	Measured parameter	Correlation coefficient (r)	$P > r$
3 Aug. 1999	Band 4	−0.61399	<0.0001
	TC-2	−0.58548	<0.0001
	TC-1	−0.56569	<0.0001
	PC-2	−0.54319	<0.0001
	PC-1	−0.53238	<0.0001
	SR	−0.49348	<0.0001
	Band 5	−0.48652	<0.0001
22 Oct. 1999	SR-Difference	−0.47574	<0.0001
	Band 5	−0.45392	<0.0001
	PC-1	−0.44102	<0.0001
	TC-1	−0.41896	<0.0001
	NDVI-Difference	−0.40946	<0.0001
	Band 7	−0.35099	<0.0001
	PC-3	−0.34489	<0.0001

Band, Landsat 7 ETM+ band values; TC, tasseled cap values; PC, principle component values; SR, simple ratio values; NDVI, normalized difference vegetation index values.

The best subset regression analysis (Ott 1993) conducted on the training sets (85% of the data points) produced models containing 12 variables (using the Landsat 7 ETM+ data from 3 August) or 19 variables (using the Landsat 7 ETM+ data from 22 October) (Table 3). Landsat bands, DOQ data, and physical parameters such as slope and elevation of the stands were common to both of the models. Based upon the R^2 and residual mean square error (RMSE) values (Table 4), the date of imagery acquisition did not seem to significantly influence the ability of the models to accurately predict the hazard value of a stand. Fur-

Table 3. Best subset regression analysis coefficient values (models) to predict southern pine beetle hazard rating scores by using the variables derived from imagery obtained from two sample dates

Date	Model parameter	Regression coefficient	Date	Model parameter	Regression coefficient
3 Aug.	Intercept	1.39858	22 Oct.	Intercept	3.77579
	Band 7	6.73794		Band 1	8.69283
	Band 4-Diff	−3.40231		Band 2	−2.37487
	TC-2	−0.03436		Band 5	−10.05809
	TC-3	0.04567		Band 4-Diff	−9.31122
	PanText5	−14.44424		SR	−0.16501
	DOQText7	0.01019		PC-2	−0.00997
	class 5	0.44948		PanText5	−27.33939
	Slope	−0.01293		DOQText7	0.00927
	Elevation	−0.00080		Slope	−0.00802
	Asp-2	0.07279		Elevation	−0.00131
	Asp-3	0.10781		Asp-1	−0.08623
				Asp-3	0.07039
				Asp-6	−0.07294
				Asp-7	−0.14689
				Asp-8	−0.15009

Model parameters are as follows: band, Landsat 7 ETM+ band values; TC, tasseled cap values; PC, principle component values; SR, simple ratio values; PanText5, 5 by 5 pixel panchromatic band texture analysis results; DOQTest7, 7 by 7 pixel standard deviation texture analysis of DOQ image; class, results of the unsupervised classification; slope, elevation, and aspect, derived from USGS DEMs with aspect (Asp) classified into eight directional classes.

thermore, the relatively small values for the RMSE (≈0.36 for both dates) suggest that the models are sensitive enough to distinguish between the three hazard classes (range 0.001–1.000 for low hazard stands, 1.001–1.500 for moderate hazard stands, and 1.501–2.200 for high hazard stands).

The hazard rating maps derived from the regression models for both dates of data acquisition have similar spatial distributions to the hazard classes derived using an inverse distance weighting technique (Fig. 2), indicating that the regression method can be used to predict hazard class for a stand. However, although there is a general similarity in the overall spatial patterns, the values for the regression model maps are determined on a pixel-by-pixel basis without any influence from neighboring pixels. Therefore, the models can be used to assign hazard values to stands that are spatially distant from the measured stands. The hazard values assigned outside of the study area will be as accurate as the values assigned to stands within the study area as long as the stands are similar in structure and terrain parameters. Most hazard maps will interpolate between measured points over a fairly large area.

Table 4. Training set and validation models along with the relevant statistics (R^2, C_p, and RMSE) derived from the best subset regression analyses conducted on the 3 August 1999 and 22 October 1999 Landsat 7 ETM+ imagery

Date	No. parameters	Training set			Validation set	
		R^2	C_p	RMSE	R^2	Cp
3 Aug.	12	0.55	12.8	0.36	0.55	0.36
22 Oct.	16	0.54	19.8	0.36	0.50	0.37

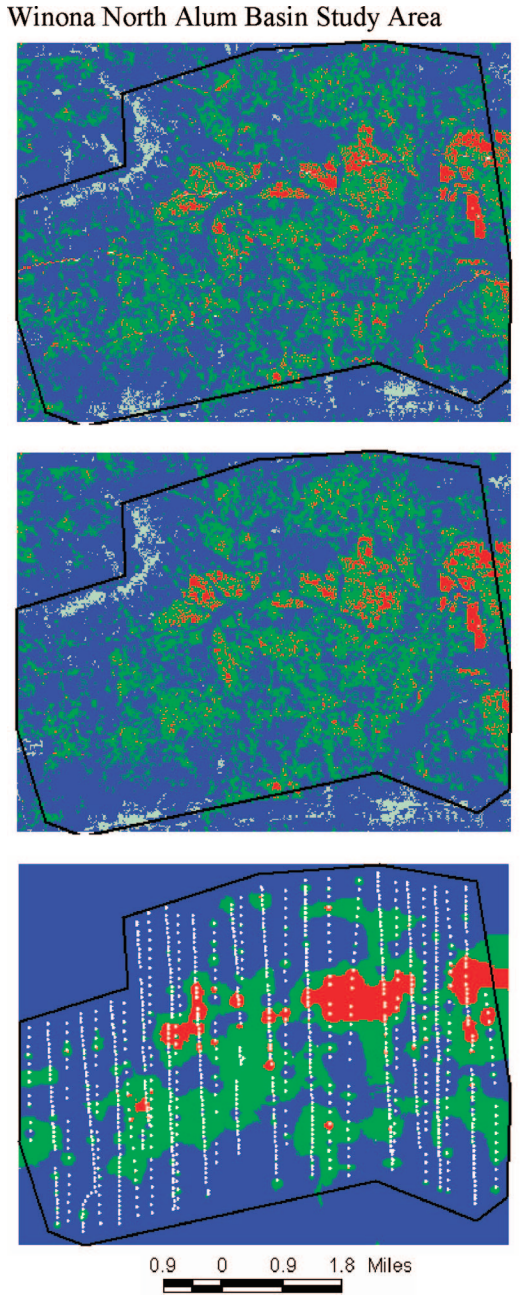

Fig. 2. Southern pine beetle hazard rating maps, where red is high hazard stands, green is moderate hazard stands, blue is low hazard stands, and gray is nonhost stands with no risk of southern pine beetle infestation. Maps are of the three watersheds contained in the North Alum Basin. The maps were constructed using the Landsat 7 ETM+ data collected on 3 August 1999 (map a), the Landsat 7 ETM+ data collected on 22 October 1999 (map b), or by interpolating the survey plot data by using an inverse distance weighted technique (map c).

Therefore, what is typically produced are large, contiguous areas all within a single hazard class, and the pixel-by-pixel differentiation of stands (Fig. 2) is not possible.

Managing forest resources to reduce the risk of insect outbreaks is a complex process that requires timely and accurate information. Hazard rating forest stands for their susceptibility to various insects could provide forest managers with one more tool to limit damage from these insects. Most of the currently used hazard rating systems for southern pine beetle use expensive and time-consuming ground surveys. New systems that integrate remotely sensed data and GIS techniques could be cost-effective, and they would aid forest managers in prescribing silvicultural treatments to be implemented to reduce losses to the beetle.

The current project examined several watersheds in the Ouachita Mountains of Arkansas. The results suggest that by combining Landsat 7 ETM+ multispectral and panchromatic band data with DOQ and terrain data for variables selected through best subset regression analyses, forest managers can produce maps with reliable estimates of hazard to southern pine beetle. After being developed, the hazard values generated from the regression procedures should be appropriate for use over similar areas. However, these hazard-rating techniques should not be expected to predict southern pine beetle activity within any given stand. The hazard maps produced during the current study used forest stand characteristics. Many of the parameters used to generate the maps are dynamic and continuously changing. The suitable habitat available to the insect can vary through time due to factors such as timber harvesting, previous herbivory, or stand growth (Coulson et al. 1999). Hazard maps therefore need to be periodically updated. Also, there are many factors that dictate whether an outbreak of southern pine beetle will occur and some of these factors cannot be detected using remotely sensed data (i.e., presence of the beetle within a stand).

Acknowledgments

This study was supported in part through a cooperative agreement between the USDA-Forest Service, Southern Research Station and the University of Idaho as part of the Ecosystem Management Research Program.

References Cited

Ahern, F., T. Erdle, D. A. MacLean, and I. D. Kneppeck. 1991. A quantitative relationship between Landsat TM spectral response and forest growth rates. Intl. J. Remote Sens. 12: 387–400.

Billings, R. F. 1988. Forecasting southern pine beetle infestation trends with pheromone traps, pp. 295–306. *In* T. L. Payne and H. Saarenmaa [eds.], Integrated control of scolytid bark beetles. Virginia Polytechnic Institute and State University, Blacksburg, VA.

Birth, G. S., and G. R. McVey. 1968. Measuring the color of growing turf with a reflectance spectrophotometer. Agron. J. 60: 640–643.

Bowers, W. W., S. E. Franklin, J. Hudak, and G. J. McDermid. 1994. Forest structural damage analysis using image semivariance. Can. J. Remote Sens. 20: 28–36.

Campbell, J. B. 1996. Introduction to remote sensing. Guilford Press, New York.

Chavez, P. S., Jr., and A. Y. Kwarteng. 1989. Extracting spectral contrast in Landsat thematic mapper image data using selective principal component analysis. Photogram. Eng. Remote Sens. 55: 339–348.

Chen, J. M. 1996. Evaluation of vegetation indices and a modified simple ratio for boreal applications. Can. J. Remote Sens. 22: 229–242.

Cohen, W. B., and T. A. Spies. 1992. Estimating structural attributes of Douglas fir/western hemlock forest stands from Landsat and SPOT imagery. Remote Sens. Environ. 41: 1–17.

Coulson, R. N. 1979. Population dynamics of bark beetles. Annu. Rev. Entomol. 24: 417–447.

Coulson, R. N., T. L. Payne, J. E. Coster, and M. W. Houseweart. 1972. The southern pine beetle, *Dendroctonus frontalis* Zimmermann (Coleoptera: Scolytidae) 1961–1971. Texas For. Serv. Publ. 108.

Coulson, R. N., B. A. McFadden, P. E. Pulley, C. N. Lovelady, J. W. Fitzgerald, and S. B. Jack. 1999. Heterogeneity of forest landscapes and the distribution and abundance of southern pine beetle. For. Ecol. Manag. 114: 471–485.

Crist, E. P., and R. C. Cicone. 1984. A physically-based transformation of thematic mapper data–the TM tasseled cap. IEEE Trans. Geosc. Remote Sens. GE-22: 256–263.

DiIorio, Frank C. 1997. SAS applications programming: a gentle introduction. Duxbury Press, Belmont, CA.

Environmental Systems Research Institute. 1997. ArcInfo, version 7.1.2. Environmental Systems Research Institute, Redlands, CA.

Environmental Systems Research Institute. 1998. ArcView, version 3.1. Environmental Systems Research Institute, Redlands, CA.

ERDAS, Inc. 1999. Imagine, version 8.4. ERDAS, Inc. Atlanta, GA.

Everitt, J. H., J. V. Richerson, J. P. Karges, and M. R. Davis. 1997a. Using remote sensing to detect and monitor a western pine beetle infestation in west Texas. Southwest. Entomol. 22: 285–292.

Everitt, J. H., J. V. Richerson, J. Karges, M. A. Alaniz, M. R. Davis, and A. Gomez. 1997b. Detecting and mapping western pine beetle infestations with airborne videography, global positioning system and geographic information system technologies. Southwest. Entomol. 22: 293–300.

Flamm, R. O., R. N. Coulson, and T. L. Payne. 1988. The southern pine beetle, pp. 531–553. *In* A. A. Berryman [ed.], Dynamics of forest insect populations. Plenum, New York.

Franklin, S. E., and J. E. Luther. 1995. Satellite remote sensing of balsam fir forest structure, growth, and cumulative defoliation. Can. J. Remote Sens. 21: 400–411.

Guldin, J. M., J. B. Baker, and M. G. Shelton. 1994. Midstory and overstory plants in mature pine-hardwood stands on south facing slopes of the Ouachita/Ozark National Forests, pp. 29–49. *In* J. B. Baker [ed.], Ecosystem management research in the Ouachita Mountains: pretreatment conditions and preliminary findings. U.S. Dep. Agric.–For. Serv. Gen. Tech. Rep. SO-112.

Hall, F. G., D. E. Strebel, J. E. Nickeson, and S. J. Goetz. 1991. Radiometric rectification: toward a common radiometric response among multidate, multisensor images. Remote Sens. Environ. 35: 11–27.

Hicks, R. R., Jr. 1980. Climate, site, and stand factors, pp. 55–68. *In* R. C. Thatcher, J. L. Searcy, J. E. Coster, and G. D. Hertel [eds.], The southern pine beetle. U.S. Dep. Agric.–For. Serv. Tech. Bull. 1631.

Hicks, R. R., Jr., J. E. Coster, and G. N. Mason. 1987. Forest insect hazard rating. J. For. 85: 20–25.

Jensen, J. R. 1996. Introductory digital image processing: a remote sensing perspective. Prentice-Hall, Upper Saddle River, NJ.

Jensen, J. R. 2000. Remote sensing of Environment: an earth resources perspective. Prentice-Hall, Upper Saddle River, NJ.

Kimes, D. S., B. N. Holben, J. E. Nickeson, and W. A. McKee. 1996. Estracting forest age in a Pacific Northwest forest from thematic mapper and topographic data. Remote Sens. Environ. 56: 133–140.

Lang, L. 1998. Managing natural resources with GIS. Environmental Systems Research Institute, Redlands, CA.

Lorio, P. L., Jr. 1978. Developing stand risk classes for the southern pine beetle. U.S. Dep. Agric.–For. Serv. Res. Pap. SO-144.

Lorio, P. L., Jr. 1980a. Loblolly pine stocking levels affect potential for southern pine beetle infestation. South. J. Appl. For. 4: 162–165.

Lorio, P. L., Jr. 1980b. Rating stands for susceptibility to SPB, pp. 153–163. *In* R. C. Thatcher, J. L. Searcy, J. E. Coster, and G. D. Hertel [eds.], The southern pine beetle. U.S. Dep. Agric.–For. Serv. Tech. Bull. 1631.

Lorio, P. L., Jr., and R. A. Sommers. 1981. Use of available resource data to rate stands for southern pine beetle risk, pp. 75–78. *In* R. L. Hedden, S. J. Barras, and J. E. Coster [eds.]. Hazard-rating systems in forest insect pest management: symposium proceedings. U.S. Dep. Agric.–For. Serv. Gen. Tech. Rep. WO-27.

Markham, B. L., and J. L. Barker. 1986. Landsat MSS and TM post-callibration dynamic ranges, exoatmospheric reflectances and at-satellite temperatures, pp. 1–5. EOSAT: Landsat technical notes, NASA.

Martin, M. E., S. D. Newman, J. D. Aber, and R. G. Congalton. 1998. Determining forest species composition using high spectral resolution remote sensing. Remote Sens. Environ. 65: 249–254.

Mather, P. M. 1996. Computer processing of remotely sensed imagery: an introduction. Wiley, New York.

Murtha, P. A., and R. J. Wiart. 1989. PC-based digital analysis of mountain pine beetle current-attacked and non-attacked lodgepole pine. Can. J. Remote Sens. 15: 70–76.

Nebeker, T. E., M. Pellegrine, R. A. Tisdale, and J. D. Hodges. 1995. Potential impact of southern pine beetle infestations on red-cockaded woodpecker colonies on the Noxubee National Wildlife Refuge: hazard rating comparison and spot growth potentials, pp. 196–207. *In* D. L. Kulhavy, R. G. Hooper, and R. Costa [eds.], Red cockaded woodpecker: recovery, ecology, and management. Stephen F. Austin University, Nacogdoches, TX.

Ott, R. L. 1993. An introduction to statistical methods and data analysis. Duxbury Press, Belmont, CA.

Payne, T. L. 1980. Life history and habits, pp. 7–28. *In* R. C. Thatcher, J. L. Searcy, J. E. Coster, and G. D. Hertel [eds.], The southern pine beetle. U.S. Dep. Agric.–For. Serv. Tech. Bull. 1631.

Rencz, A. N., and J. Nemeth. 1985. Detection of mountain pine beetle infestation using Landsat MSS and simulated thematic mapper data. Can. J. Remote Sens. 11: 50–58.

Robinove, C. J. 1982. Computation and physical values from Landsat digital data. Photogram. Eng. Remote Sens. 48: 781–784.

Rouse, J. W. R., H. Haas, J. A. Schell, and D. W. Deering. 1974. Monitoring vegetation systems in the Great Plains with ERTS. *In* Proceedings of the 3rd Earth Resource Technology Satellite (ERTS) Symposium. NASA Special Publication No. 356, 1: 48–62.

SAS Institute. 2000. Statistical analysis system, version 8.1. SAS Institute, Cary, NC.

St. George, R. A., and J. A. Beal. 1929. The southern pine beetle: a serious enemy of pines in the south. U.S. Dep. Agric. Farmers Bull. 1586.

Received 16 November 2004; accepted 26 November 2006.